DOI:10.22337/2587-9618-2025-21-1-93-104

FEATURES OF MODELING THE OPERATION OF REINFORCED CONCRETE STRUCTURES USING INCONSISTENT FINITE ELEMENT MODELS

Ivan V. Nesterov, Ksenia K. Pantyukhova, Elizabeth A. Sheiko

Russian University of Transport (MIIT), Moscow, RUSSIA

Abstract: This article is devoted to the development of inconsistent finite element models of reinforcing rods for strength analysis of reinforced concrete structures. Currently, reinforcement in the calculations of reinforced concrete structures is taken into account using various methods. The authors pay special attention to the embedded finite element model. The article discusses mathematical models and technology for the output of stiffness matrices of reinforcing rods embedded in finite elements of various configurations. Using the derived finite elements, a number of comparative test calculations of reinforced concrete beams were carried out. Numerical solutions on inconsistent FE grids were compared with the results obtained on a consistent finite element grid.

Keywords: finite element method, reinforced concrete structures, consistent finite element model, inconsistent finite element model, reinforcement, discrete model, simplex element, plate element

ОСОБЕННОСТИ МОДЕЛИРОВАНИЯ РАБОТЫ ЖЕЛЕЗОБЕТОННЫХ КОНСТРУКЦИЙ С ИСПОЛЬЗОВАНИЕМ НЕСОГЛАСОВАННЫХ КОНЕЧНО-ЭЛЕМЕНТНЫХ МОДЕЛЕЙ

И.В. Нестеров, К.К. Пантюхова, Е.А. Шейко

Российский университет транспорта (МИИТ), г. Москва, РОССИЯ

Аннотация: Данная статья посвящена разработке несогласованных конечно-элементных моделей арматурных стержней для прочностного анализа железобетонных конструкций. В настоящее время арматура в расчётах железобетонных конструкциях учитывается с помощью разных методов. Особое внимание авторы уделят встроенной конечно-элементной модели. В статье рассматриваются математические модели и технология вывода матриц жесткости арматурных стержней, встроенных в конечные элементы различной конфигурации. С использованием выведенных конечных элементов был проведен ряд сравнительных тестовых расчетов железобетонных балок. Численные решения на несогласованных сетках КЭ сравнивались с результатами, полученными на согласованных сетках конечных элементов.

Ключевые слова: метод конечных элементов, железобетонные конструкции, согласованная конечно-элементная модель, несогласованная конечно-элементная модель, арматура, дискретная модель, симплекс-элемент, пластинчатый элемент

INTRODUCTION

Currently, reinforced concrete structures are widely used in the construction industry. Reinforced concrete is a complex composite material for strength analysis. Therefore, when calculating this class of structures, it is necessary to take into account such factors as creep, shrinkage, nonlinear deformations from the acting load, etc. One of the main problems that arise when calculating reinforced concrete structures is modeling the interaction of the reinforcement frame and concrete.

There are different methods for calculating reinforced concrete structures. The finite element method (FEM) is the most common among designers for studying the stress-strain state of a structure [1]. The finite element method is implemented in many software packages used for strength analysis of engineering structures. It is worth highlighting the most popular of them: Midas, Abaqus, ANSYS, Sofistik, Scad, etc.

The joint work of reinforcement and concrete in finite element models is taken into account in different ways. The most common, simple and affordable method is to recalculate the given physical characteristics of concrete, taking into account the percentage of reinforcement according to standard SNiP methods. Calculation recommendations are specified in SP 63.13330.2018 "Concrete and reinforced concrete structures" [2], as well as in the methodological guide for the calculation of reinforced concrete elements "Methodological recommendations for the use of SP 35.13330.2011" [3]. This method of accounting for fittings is convenient for standard (simple) cross-sections. In a complex section, when reduced to an equivalent one, the stress distribution may differ significantly from the real picture of the stress-strain state. The most accurate method is to create a discrete model based on consistent finite element grids (FE). In this simulation, the nodes of the reinforcing rods coincide with the nodes of the concrete component (Fig. 1).

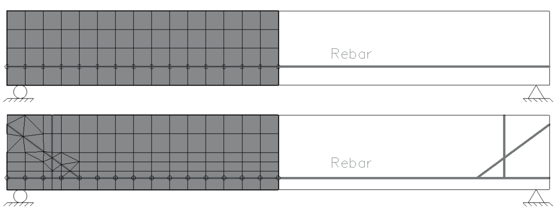

Figure 1. Discrete model on matched FE grids

However, the process of creating such a design scheme is very laborious. The reinforcement frame can consist of different types of rods having different positions, lengths, etc. For example, there may be horizontal, vertical, and inclined rods in one design scheme. During the design process, the configuration (parameters) of the beams and reinforcement frame often change. Accordingly, each time you will have to redo the calculation scheme. Therefore, it is impractical to use a consistent finite element model for such tasks. Basically, this model is applicable for simple reinforcement frames, or for test calculations.

Methods that do not require consistency of the grid nodes, the concrete component, and the reinforcement frame are more convenient for calculation. One of these is a discrete model using scalable contour lines [4]. With this method, the initial model is discretized. The finite elements through which the reinforcement passes are divided into subdomains in the form of polyhedra (Fig. 2).

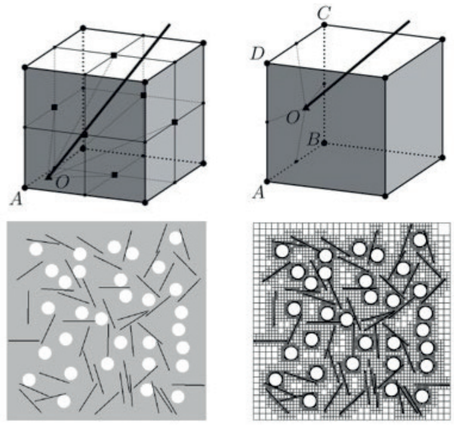

Figure 2. Discrete model using scalable contour lines [4]

There is also a distributed FE model, which also does not require the consistency of FE nodes [5]. In this method, the reinforcement is modeled as thin plates that are “stretched” onto the plates of the concrete component through which the rod passes. An anisotropic plate is obtained. This technology is implemented in the Abaqus and Ansys software packages. Currently, embedded finite element models are being intensively developed [6,7], which make it possible to accurately take into account the influence of reinforcement in the design scheme of reinforced concrete structures, without worrying about matching the grid nodes of the concrete component and the reinforcement frame. This approach is convenient for software users, but for software developers there are difficulties associated with the need to create an additional library of finite elements and make adjustments to the architecture of the software package. This model is most fully implemented in the Midas software package. In domestic strength analysis systems, the embedded model is insufficiently developed and requires a full-fledged software implementation.

A GENERAL ALGORITHM FOR THE FORMATION OF FINITE ELEMENT STIFFNESS MATRICES FOR AN EMBEDDED FE MODEL OF REINFORCED CONCRETE

The theoretical basis of the integrated reinforcement accounting model is the hypothesis of the compatibility of concrete and reinforcement deformations, as a result of which nodal reactions are added to the nodal reactions of the plate element from single displacements according to degrees of freedom from deformation of the reinforcing rod in the contour of the plate, but not from single displacements of the rod nodes, but from single displacements of the plate nodes through which it passes (3). This additive is calculated using the integral over the length of the embedded rod.

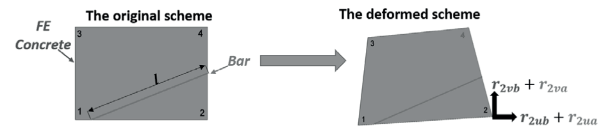

Figure 3. Deformation of a plate finite element with an integrated reinforcing rod

Thus, based on the hypothesis of joint deformations of concrete and reinforcement, the field of displacement of the reinforcing rod is actually a cross-section of the field of displacement of the plate. Based on this, the reaction matrix of a plate element with an integrated reinforcing rod can be obtained by the formula (1).

$$r = \int_V \sigma^T \varepsilon \, dV + \int_l \sigma^T \varepsilon \, dl = \int_V B^T D B \, dV + \\ +F \int_l B_a^T E B_a \, dl, \qquad (1)$$

Where B - is the deformation matrix of the plate element (concrete),

D - is the matrix of Hooke's law [8],

B_a- reinforcement deformation matrix,

F_a - is the cross-sectional area of the reinforcement.

Using this approach, several finite elements were derived: a triangular simplex element, a 4-node plate FE, a 9-node plate FE, and a bending plate.

OUTPUT OF THE STIFFNESS MATRIX OF A TRIANGULAR SIMPLEX ELEMENT WITH AN INTEGRATED REINFORCING ROD

Using the above algorithm, we obtain a stiffness matrix for a triangular simplex element with an integrated reinforcing rod. For a triangular finite element, the basic functions are the equations of the plane, respectively, the displacement field is a function of two variables (2).

$$\vec{z}(x) = \left[\begin{matrix} n_1(xy) & 0 \\ 0 & n_1(xy) \end{matrix}\middle|\begin{matrix} n_2(xy) & 0 \\ 0 & n_2(xy) \end{matrix}\middle| \\ \middle|\begin{matrix} n_3(xy) & 0 \\ 0 & n_3(xy) \end{matrix}\right] \vec{z} \qquad (2)$$

In order to obtain the displacement field (3) for the embedded reinforcing rod in the triangle, it is necessary to switch to the local coordinate system of the rod.

$$\vec{z}(x) = \left[\begin{matrix} nl_1(x) & 0 \\ 0 & nl_1(x) \end{matrix}\middle|\begin{matrix} nl_2(x) & 0 \\ 0 & nl_2(x) \end{matrix}\middle| \\ \middle|\begin{matrix} nl_3(x) & 0 \\ 0 & nl_3(x) \end{matrix}\right] \vec{z} \qquad (3)$$

This makes it possible to obtain the displacement field of the embedded rod by a set of functions of one variable, which are sections of functions of the triangle shape (4) (Fig.4).

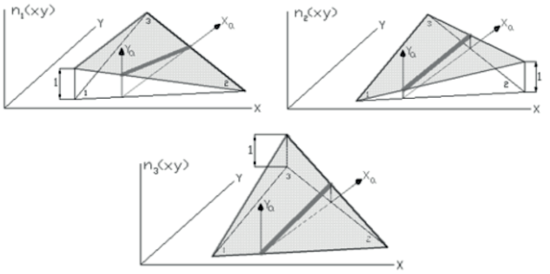

Figure 4. Basic functions of an embedded reinforcing bar in a triangle

$$nl_1(x) = \frac{(-a_1 \cdot xx - c_1)}{b_1},$$
$$nl_2(x) = \frac{(-a_2 \cdot xx - c_2)}{b_2},$$
$$nl_3(x) = \frac{(-a_3 \cdot xx - c_3)}{b_3}, \qquad (4)$$

Where a_1, a_2, a_3, b_1, b_2, b_3, c_1, c_2, c_3, xx - parameters of the direct line

The embedded reinforcing rod in the plate element has its own tilt angle relative to the global coordinate system (Fig.5), therefore, the stiffness matrix of the embedded element must be multiplied by the rotation matrix (5).

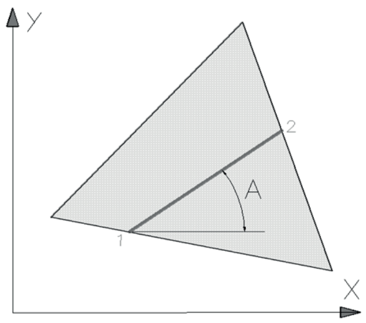

Figure 5. Tilt angle of the embedded rod

$$C = \begin{bmatrix} CA & 0 & 0 \\ 0 & CA & 0 \\ 0 & 0 & CA \end{bmatrix}, CA = \begin{bmatrix} cosA & sinA \\ -sinA & cosA \end{bmatrix} \qquad (5)$$

The final stiffness matrix of a triangular simplex element with an integrated reinforcing rod is obtained by summing the stiffness matrix of a triangular plate element and the reinforcement matrix (6).

$$r = \frac{\delta}{F_{\text{тр}}} B^T DB + C^T [FlB_a^T E_a B_a] C, \qquad (6)$$

Where B - is the deformation matrix of the plate element (concrete),

B_a - is the deformation matrix of the reinforcement,

C - is the matrix of transition to the local coordinate system of the rod (5),

D - is the matrix of Hooke's law [8],

F - is the cross-sectional area of the reinforcement.

OUTPUT OF THE STIFFNESS MATRIX OF A FLAT QUADRILATERAL WITH AN INTEGRATED REINFORCING ROD

In a similar way, a stiffness matrix was obtained for a four-node plane FE with an embedded reinforcing rod. The basic functions of a flat quadrilateral are linear surfaces, so the displacement field is also a function of two variables (7).

$$\vec{z}(x) = \begin{bmatrix} n_1(xy) & 0 \\ 0 & n_1(xy) \end{bmatrix} \begin{vmatrix} n_2(xy) & 0 \\ 0 & n_2(xy) \end{vmatrix} \begin{vmatrix} n_3(xy) & 0 \\ 0 & n_3(xy) \end{vmatrix} \begin{bmatrix} n_4(xy) & 0 \\ 0 & n_4(xy) \end{bmatrix} \vec{z} \qquad (7)$$

To obtain the stiffness matrix based on the embedded rod, it is necessary to switch to the local coordinate system of the rod. Thus, the displacement field of the embedded reinforcing rod (8) becomes a function of one variable.

$$\vec{z}(x) = \begin{bmatrix} nl_1(x) & 0 \\ 0 & 0 \end{bmatrix} \begin{vmatrix} nl_2(xy) & 0 \\ 0 & 0 \end{vmatrix} \begin{vmatrix} nl_3(x) & 0 \\ 0 & 0 \end{vmatrix} \begin{bmatrix} nl_4(x) & 0 \\ 0 & 0 \end{bmatrix} \vec{z} \qquad (8)$$

The basic functions for an embedded reinforcing bar in a flat quadrilateral are shown below (Fig.6) (9):

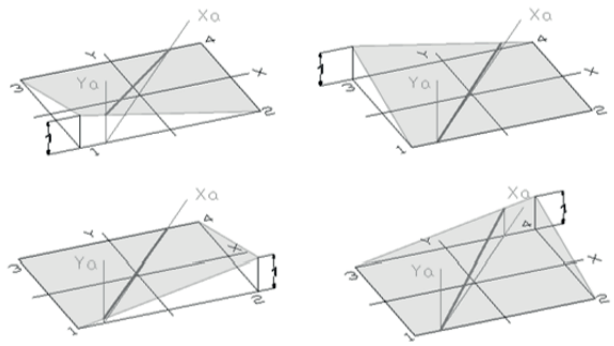

Figure 6. Basic functions of an embedded reinforcing bar in a flat quadrilateral

$$nl_1(x) = \left(\frac{1}{2} - \frac{cosAdl + x1}{a}\right)\left(\frac{1}{2} - \frac{sinAdl + y1}{b}\right),$$
$$nl_2(x) = \left(\frac{1}{2} + \frac{cosAdl + x1}{a}\right)\left(\frac{1}{2} - \frac{sinAdl + y1}{b}\right),$$
$$nl_3(x) = \left(\frac{1}{2} - \frac{cosAdl + x1}{a}\right)\left(\frac{1}{2} + \frac{sinAdl + y1}{b}\right),$$
$$nl_4(x) = \left(\frac{1}{2} + \frac{cosAdl + x1}{a}\right)\left(\frac{1}{2} + \frac{sinAdl + y1}{b}\right), \qquad (9)$$

Where dl - is the parameter of the line,
$a,\ b$ - are the dimensions of the sides of a flat quadrangle,
$x1,\ y1$ - is the initial coordinate of the reinforcing bar.
The reinforcing bar embedded in the rectangle relative to the global coordinate system is rotated by an angle A (Fig.7).

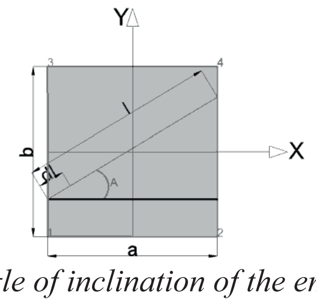

Figure 7. Angle of inclination of the embedded rod

The stiffness matrix of the rod must be multiplied by the cosine matrix consisting of diagonal blocks (10).

$$C = \begin{bmatrix} CA & 0 & 0 & 0 \\ 0 & CA & 0 & 0 \\ 0 & 0 & CA & 0 \\ 0 & 0 & 0 & CA \end{bmatrix}, CA = \begin{bmatrix} cosA & sinA \\ -sinA & cosA \end{bmatrix} \quad (10)$$

The final stiffness matrix of the plate four-node FE, taking into account the reinforcement, is obtained by summing the local stiffness matrix of the plate element (concrete component) and the matrix of the embedded reinforcing rod according to the formula (11).

$$r = \delta \int_{-\frac{a}{2}}^{\frac{a}{2}} \int_{-\frac{b}{2}}^{\frac{b}{2}} B^T DB\, dx\, dy + C^T \left[F_a \int_0^l B_a^T E B_a\, dx_a \right] C, \qquad (11)$$

Where B - is the deformation matrix of the plate element (concrete),
B_a - is reinforcement deformation matrix,
C - is the matrix of transition to the local coordinate system of the rod (10),
D - is the matrix of Hooke's law [8],
F_a - is the cross-sectional area of the reinforcement.

OUTPUT OF THE STIFFNESS MATRIX OF A FLAT 9-NODE QUADRILATERAL WITH AN INTEGRATED REINFORCING ROD

The stiffness matrix of a flat 9-node quadrilateral with an integrated reinforcing rod is derived according to the principle of triangular and four-node finite elements. In this case, only the basic functions are second-order surfaces. Accordingly, the displacement field for a 9-node element is a dependence of two variables (12).

$$\vec{z}(x) = \begin{bmatrix} n_1(xy) & 0 \\ 0 & n_1(xy) \end{bmatrix} |\dots| \begin{vmatrix} n_9(xy) & 0 \\ 0 & n_9(xy) \end{vmatrix} \vec{z} \qquad (12)$$

To obtain the stiffness matrix of a 9-node plate core with an integrated reinforcing rod, it is necessary to switch to the local coordinate system of the rod. For a reinforcing bar, the displacement field is a cross-section of the shape functions of a 9-node finite element and is a function of one variable (13).

$$\vec{z}(x) = \begin{bmatrix} nl_1(x) & 0 \\ 0 & 0 \end{bmatrix} \Big| \ldots \Big| \begin{bmatrix} nl_9(x) & 0 \\ 0 & 0 \end{bmatrix} \vec{z} \quad (13)$$

The basic functions for an integrated reinforcing rod in a flat 9-node plate FE are shown below (Fig.8) (14):

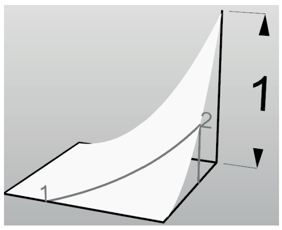

Figure 8. Example of the basic function of an embedded reinforcing bar in a 9-node quadrilateral

$$nl_1(x) = \left(-\frac{4(cosAdl + x1)^2}{a^2} + 1\right)\left(-\frac{4(sinAdl + y1)^2}{b^2} + 1\right),$$

$$nl_2(x) = \left(\frac{2(cosAdl + x1)^2}{a^2} - \frac{cosAdl + x1}{a}\right)\left(\frac{2(sinAdl + y1)^2}{b^2} - \frac{sinAdl + y1}{b}\right),$$

$$nl_3(x) = \left(\frac{2(cosAdl + x1)^2}{a^2} + \frac{cosAdl + x1}{a}\right)\left(\frac{2(sinAdl + y1)^2}{b^2} - \frac{sinAdl + y1}{b}\right),$$

$$nl_4(x) = \left(\frac{2(cosAdl + x1)^2}{a^2} - \frac{cosAdl + x1}{a}\right)\left(\frac{2(sinAdl + y1)^2}{b^2} + \frac{sinAdl + y1}{b}\right),$$

$$nl_5(x) = \left(\frac{2(cosAdl + x1)^2}{a^2} + \frac{cosAdl + x1}{a}\right)\left(\frac{2(sinAdl + y1)^2}{b^2} + \frac{sinAdl + y1}{b}\right),$$

$$nl_6(x) = \left(-\frac{4(cosAdl + x1)^2}{a^2} + 1\right)\left(\frac{2(sinAdl + y1)^2}{b^2} - \frac{sinAdl + y1}{b}\right),$$

$$nl_7(x) = \left(\frac{2(cosAdl + x1)^2}{a^2} + \frac{cosAdl + x1}{a}\right)\left(-\frac{4(sinAdl + y1)^2}{b^2} + 1\right),$$

$$nl_8(x) = \left(-\frac{4(cosAdl + x1)^2}{a^2} + 1\right)\left(\frac{2(sinAdl + y1)^2}{b^2} + \frac{sinAdl + y1}{b}\right),$$

$$nl_9(x) = \left(\frac{2(cosAdl + x1)^2}{a^2} - \frac{cosAdl + x1}{a}\right)\left(-\frac{4(sinAdl + y1)^2}{b^2} + 1\right), \quad (14)$$

Where dl - is the parameter of a straight line that takes any real values,

$a,\ b$ - are the dimensions of the sides of a flat quadrangle,

$x1,\ y1$ - is the initial coordinate of the reinforcing bar.

Also, as with the previous elements, the embedded rod has an angle of inclination A (Fig.9), therefore it is multiplied by the cosine matrix (15).

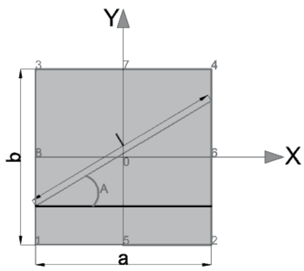

Figure 9. Angle of inclination of the embedded rod

$$C = \left[\begin{pmatrix} CA & \cdots & 0 \\ \vdots & \ddots & \vdots \\ 0 & \cdots & CA \end{pmatrix}\right], CA = \begin{bmatrix} cosA & sinA \\ -sinA & cosA \end{bmatrix} \quad (15)$$

The final stiffness matrix of the plate 9-node FE, taking into account the reinforcement, is obtained by summing the local stiffness matrix of the plate element and the matrix of the embedded reinforcing rod according to the formula (16).

$$r = \delta \int_{-\frac{a}{2}}^{\frac{a}{2}} \int_{-\frac{b}{2}}^{\frac{b}{2}} B^T D B \, dx \, dy + C^T \left[F_a \int_0^l B_a^T E B_a \, dx_a \right] C, \qquad (16)$$

OUTPUT OF THE STIFFNESS MATRIX OF A BENDING QUADRILATERAL WITH AN INTEGRATED REINFORCING ROD

The output of the stiffness matrix of a bending quadrilateral with an integrated reinforcing rod differs from the previous elements. In this element, the basic functions are second-order surfaces. The displacement field is obtained from the following relation (16):

$$z(xy) = \begin{bmatrix} w(xy) \\ \dfrac{\partial w(xy)}{\partial y} \\ -\dfrac{\partial w(xy)}{\partial x} \end{bmatrix} = L(xy)\vec{\alpha} \qquad (16)$$

The reinforcement in the bending quadrangular element is modeled using rigid links [9]. The matrix of rigid insertion (15):

$$V = \begin{bmatrix} V_{н} & 0 \\ 0 & V_{к} \end{bmatrix}, V_{н} = \begin{bmatrix} 1 & 0 & 0 \\ e_{н} & 1 & 0 \\ 0 & 0 & 1 \end{bmatrix},$$

$$V_{к} = \begin{bmatrix} 1 & 0 & 0 \\ e_{к} & 1 & 0 \\ 0 & 0 & 1 \end{bmatrix}, \qquad (15)$$

Where V - the matrix of rigid insertion,

$e_{н}$, $e_{к}$ - height of the rigid insert.

For the reinforcing rod, the stiffness matrix of the rod embedded in a flat quadrilateral is used. This matrix is then multiplied by a matrix of rigid inserts on both sides (15). The final stiffness matrix of a bending quadrilateral with an integrated reinforcing bar is obtained by adding the stiffness matrix of the bending plate and the stiffness matrix of the reinforcing bar, taking into account the rigid inserts (16).

$$r = \frac{\delta^3}{12} (L^{-1})^T \iint B^T D B \, dx \, dy L^{-1} + V^T C^T \left[F_a \int_0^l B_a^T E_a B_a \, dx_a \right] C V \qquad (16)$$

TESTING OF FINITE ELEMENTS WITH INTEGRATED REINFORCEMENT ROD

For strength calculations of reinforced concrete structures based on the embedded FE model, the authors developed a C++ program that includes a library with the finite elements described above. Test calculations of beams with reinforcing rods were performed. A beam with the following geometric characteristics was accepted for calculation: height - 14, length - 102.5, thickness -11.5. All dimensions are indicated in cm. A four-point loading scheme was used for calculations (Fig. 10). The physical characteristics of concrete and reinforcement are indicated in the calculation scheme (Fig. 10).

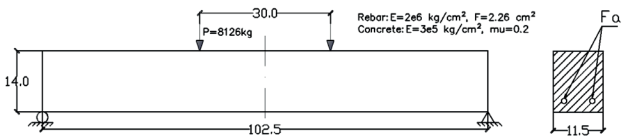

Figure 10. Calculation scheme

The comparison of the results obtained on the inconsistent meshes of the FE (the left part of the beam) was performed with the model on the consistent meshes of the FE (the right part of the beam). The model based on matched grids is calculated in the KATRAN software package.

Test-1

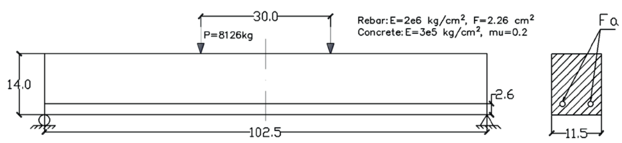

Figure 11. Calculation scheme

The first test calculations were performed on grids with triangular finite elements. The first calculation was performed on a relatively coarse mesh with a single reinforcing rod (Fig. 12). The results are shown in Table 1.

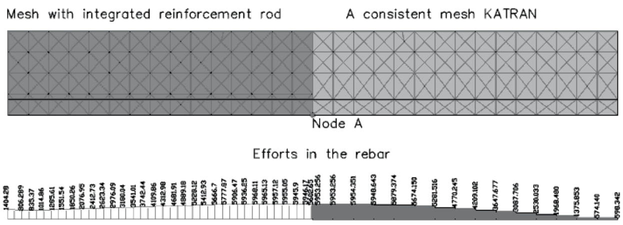

Figure 12. Finite element model and reinforcement forces on a sparse grid

In the second test calculation, the grid was thickened by 2 times (Fig. 13). The position of the reinforcing rod in the design scheme remains the same. The results are shown in the table 2.

Table 1

Criteria	Inconsistent model	A consistent model	Error rate, %
Displacement at node A (middle of the beam), cm	0.378035	0.3794	0.36
Effort, kg	5602.65	5953.26	5.89

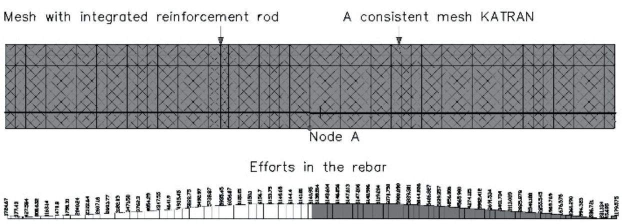

Figure 13. A finite element model and reinforcement forces on a dense grid

Table 2

Criteria	Inconsistent model	A consisten t model	Error rate, %
Displacemen t at node A (middle of the beam), cm	0.394302	0.39465	0.088
Effort, kg	6140.95	6138.514	0.0397

Test-2

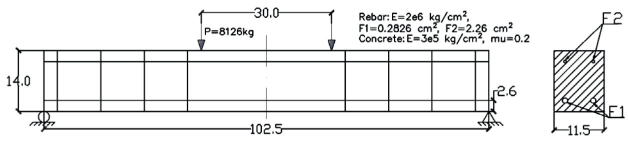

Figure 14. Calculation scheme

In the next test, a reinforcement frame with horizontal and vertical rods was added to the design scheme (Fig. 14). The results are shown in Table 3. (Fig. 15)

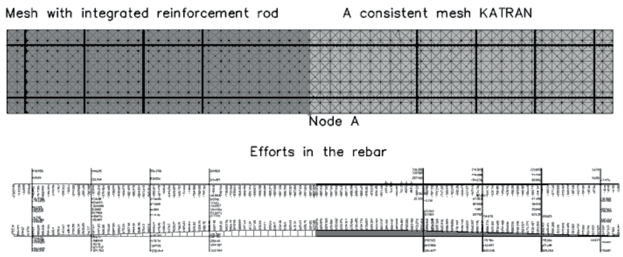

Figure 15. A finite element model with a reinforcing frame

Table 3

Criteria	Inconsisten t model	A consistent model	Error rate, %
Displacemen t at node A (middle of the beam), cm	0.389066	0.38933	0.0678
Efforts in the upper bar, kg	887.339	887.23	0.0123
Efforts in the lower bar, kg	6127.89	6125.876	0.0329
Efforts in vertical bar, kg	339.589	330.588	2.7

Test-3

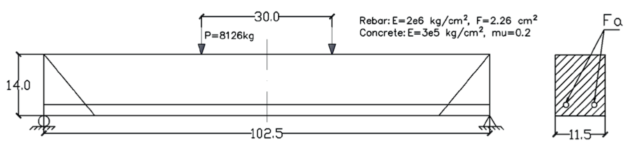

Figure 16. Calculation scheme

A four-cornered flat plate element with an integrated reinforcing rod.

Testing was performed for a beam with the same geometry as in the previous calculation (Fig. 16). But inclined reinforcing rods were added to the design scheme. The results are shown in table 4. (Fig. 17)

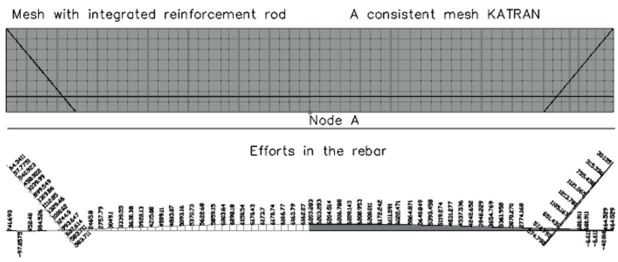

Figure 17. *A finite element model with an inclined bar*

Table 4

Criteria	Inconsistent model	A consistent model	Error rate, %
Displacement at node A (middle of the beam), cm	0.395492	0.39983	1.08
Efforts in the lower bar, kg	6162.27	6203.283	0.66
Efforts in the inclined rod, kg	583.711	574.792	1.5

Test-4

A beam with a reinforcing frame was also calculated. The calculation scheme is fully consistent (Fig. 14). The results are shown in Table 5 (Fig.18).

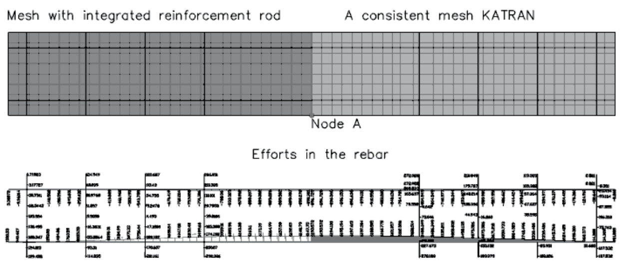

Figure 18. *A finite element model with a reinforcing frame*

Table 5

Criteria	Inconsistent model	A consistent model	Error rate, %
Displacement at node A (middle of the beam), cm	0.390491	0.39429	0.96
Efforts in the upper bar, kg	890.381	896.729	0.71
Efforts in the lower bar, kg	6147.75	6193.572	0.74
Efforts in vertical bar, kg	266.051	272.928	2.5

Test-5

A flat 9-node quadrilateral with a embedded reinforcing rod.

Based on this type of FE, a beam with a reinforcing frame was calculated (Fig. 14). The calculation results are shown in Table 6 (Fig. 19).

Table 6

Criteria	Inconsistent model	A consistent model	Error rate, %
Displacement at node A (middle of the beam), cm	0.39667	0.39429	0.6
Efforts in the upper bar, kg	896.003	896.729	0.081
Efforts in the lower bar, kg	6189.72	6193.572	0.062
Efforts in vertical bar, kg	240.527	272.928	11.87

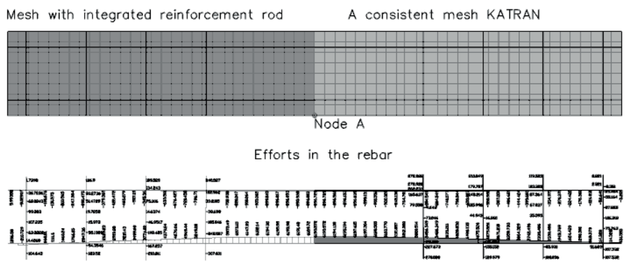

Figure 19. *Finite element model with reinforcement frame*

Test-6

A bending quadrilateral with a embedded reinforcing rod.

To test the bending plate with an integrated reinforcing bar, a spatial model with a T-shaped cross-section was created. The section parameters are shown in the figure (Fig. 20). The length of the beam is 500 cm. Reinforcement rods are located in the upper and lower parts of the beam. The physical characteristics of the materials have not changed.

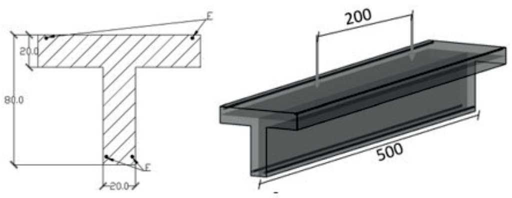

Figure 20. Cross-section profile of the T-beam

To verify the results, a calculation was performed with a model on a consistent grid (Fig.21), where rigid inserts are an element of great rigidity, with which the reinforcement rod is connected to the plate model (Fig. 22, the right part of the beam).

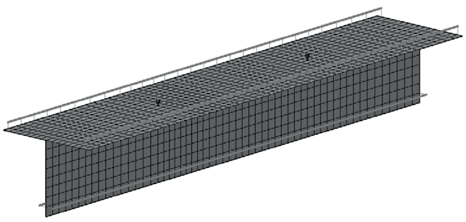

Figure 21. A finite element model with an armature frame on mismatched gridsax

The calculation results are shown in Table 7 (Fig. 22).

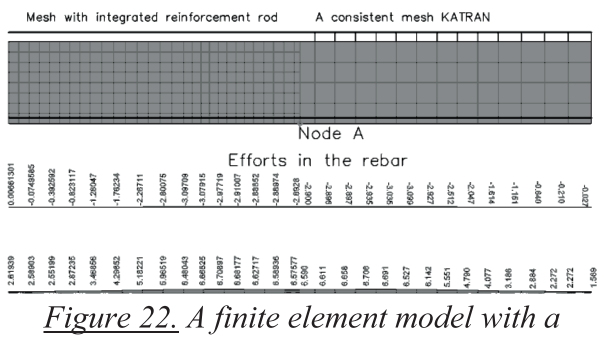

Figure 22. A finite element model with a reinforcing frame

Table 7

Criteria	Inconsistent model	A consistent model	Error rate, %
Displacement at node A (middle of the beam), cm	9.37E-04	9.54E-04	1.8
Efforts in the upper bar, kg	2.8928	2.9	0.24
Efforts in the lower bar, kg	6.57577	6.59	0.22

CONCLUSION

The method of constructing finite element models of reinforced concrete structures using embedded rod finite elements based on the hypothesis of compatibility of the deformation field of reinforcement and concrete has been improved.

The stiffness matrices of flat and flexural plate finite elements with the inclusion of reinforcing rods inconsistent with the nodes of the main grid of the FE were verified and tested.

A software package has been developed that implements finite element models of reinforced concrete structures with integrated reinforcement.

Based on a series of test calculations, a comparative analysis of coordinated and uncoordinated FE models of reinforced concrete structures was carried out, which showed high accuracy of finite element models with integrated reinforcing rods.

REFERENCES

1. **Gallagher R.**, Finite element method. Fundamentals: Translated from English– Moscow: Mir, 1984– 428 p.
2. SP 63.13330.2018. A set of rules. Concrete and reinforced concrete structures. (2019). Moscow: Standartinform.

3. Methodological recommendations for the application of SP 35.13330.2011. (2017). Moscow: Standartinform
4. **Zhang J., Eisenträger J., Duczek S., Song C**. Discrete modeling of fiber reinforced composites using the scaled boundary finite element method//Composite Structures. 2019. Vol.235. Pp.1-37
5. **Fialko S.Y.** Four-node finite element for modeling the behavior of thin-walled reinforced concrete structures // Magazine of Civil Engineering, No.5,2014, 27-36 p.
6. **Klovanich S.F.,** Finite element method in nonlinear problems of engineering mechanics: IPO LLC Zaporizhia", 2009, 400 p.
7. **Jendele L., Cˇervenka J**. On the solution of multi-point constraints – application to FE analysis of reinforced concrete structures // Computers&Structures. 2009. Vol.87. Pp. 970-980.
8. **Darkov A.V., Shaposhnikov N.N.,** Construction mechanics: Textbook.for builds. spec of universities. - M.: Higher School, 1986. – 607 p.
9. **Smirnov A.F., Alexandrov A.V., Lashchenikov B.Y., Shaposhnikov N.N.,** Construction mechanics: Textbook for universities, Moscow: Stroyizdat, 1981– 512 p.

СПИСОК ЛИТЕРАТУРЫ

1. **Галлагер Р.**, Метод конечных элементов. Основы: Пер. с англ. – М.: Мир, 1984. – 428 с.
2. СП 63.13330.2018. Свод правил. Бетонные и железобетонные конструкции. (2019). М.: Стандартинформ
3. Методическое пособие. Методические рекомендации по применению СП 35.13330.2011. (2017). М.: Стандартинформ
4. **Zhang J., Eisenträger J., Duczek S., Song C**. Discrete modeling of fiber reinforced composites using the scaled boundary finite element method//Composite Structures. 2019. Vol.235. Pp.1-37
5. **Фиалко С.Ю**. Четырехузловой конечный элемент для моделирования поведения тонкостенных железобетонных конструкций // Magazine of Civil Engineering, No.5, 2014, 27-36 с.
6. **Клованич С.Ф.**, Метод конечных элементов в нелинейных задачах инженерной механики: ООО "ИПО" Запорожье", 2009, 400 с.
7. **Jendele L., Cˇervenka J**. On the solution of multi-point constraints – application to FE analysis of reinforced concrete structures // Computers&Structures. 2009. Vol.87. Pp. 970-980.
8. **Дарков А.В., Шапошников Н.Н.**, Строительная механика: Учеб.для строи. спец вузов. - М.: Высш. Шк., 1986. – 607 с.
9. **Смирнов А.Ф., Александров А.В., Лащеников Б.Я., Шапошников Н.Н.**, Строительная механика: Учеб. для вузов - М.: Стройиздат, 1981. – 512 с.

Ivan V. Nesterov, Associate Professor, Ph.D, Associate Professor of «Computer Aided Design» Department, Institute of Railway Track, Construction and Structures, Russian University of Transport (MIIT), 127994, GSP-4, Moscow, Obraztsova str., 9, building 9, e-mail: saprforever@gmail.com

Ksenia K. Pantyukhova, Master's Student at the Russian University of Transport (MIIT), specialist of the Center for Integrated Projects of Management of New Projects and Technologies of the Russian University of Transport (MIIT), a leading engineer of the design department of LLC «Intermost», 127994, GSP-4, Moscow, Obraztsova str., 9, building 9, e-mail: ksushap13.03.2001@mail.ru

Elizabeth A. Sheiko, Assistant of «Computer Aided Design» Department, Institute of Railway Track, Construction and Structures, Russian University of Transport (MIIT), 127994, GSP-4, Moscow, Obraztsova str., 9, building 9, e-mail: elizabet-250997@mail.ru

Нестеров Иван Владимирович, доцент, кандидат технических наук, доцент кафедры «Системы автоматизированного проектирования» Института пути, строительства и сооружений Российского университета транспорта (МИИТа), 127994, ГСП-4, Москва, ул. Образцова, д.9, стр. 9, e-mail: saprforever@gmail.com

Пантюхова Ксения Константиновна, магистрант Российского университета транспорта (МИИТа), специалист Центра комплексных проектов Управления новых проектов и технологий Российского университета транспорта (МИИТа), ведущий инженер отдела проектирования ООО «Интермост», 127994, ГСП-4, Москва, ул. Образцова, д.9, стр. 9, e-mail: ksushap13.03.2001@mail.ru

Шейко Елизавета Алексеевна, ассистент кафедры «Системы автоматизированного проектирования» Института пути, строительства и сооружений Российского университета транспорта (МИИТа), 127994, ГСП-4, Москва, ул. Образцова, д.9, стр. 9, e-mail: elizabet-250997@mail.ru